Alkaline Earth Compounds | Hot Paper

Deutsche Ausgabe: DOI: 10.1002/ange.201914986
Internationale Ausgabe: DOI: 10.1002/anie.201914986

A Stable Calcium Alumanyl

Ryan J. Schwamm, Martyn P. Coles, Michael S. Hill, Mary F. Mahon, Claire L. McMullin,* Nasir A. Rajabi, and Andrew S. S. Wilson*

Abstract: *A seven-membered N,N′-heterocyclic potassium alumanyl nucleophile is introduced and utilised in the metathetical synthesis of Mg–Al and Ca–Al bonded derivatives. Both species have been characterised by experimental and theoretical means, allowing a rationalisation of the greater reactivity of the heavier group 2 species implied by an initial assay of their reactivity.*

Alkaline earth (Ae = Be, Mg, Ca, Sr, Ba) compounds continue to provide unprecedented observations for stoichiometric and catalytic bond activation.[1] Some of the most notable advances have been provided by kinetically-stabilized hydride derivatives.[2] The β-diketiminato calcium complex, $[(^{Dipp}BDI)CaH]_2$ (**1**, $^{Dipp}BDI = HC\{(Me)CNDipp\}_2$; Dipp = 2,6-*i*-$Pr_2C_6H_3$), for example, reacts with alkenes to provide *n*-alkyl derivatives, which are sufficiently reactive to effect even the nucleophilic alkylation of benzene.[3] These observations also impel the exploration of a broader range of Ae–X bonded compounds. A topical case in point is provided by reports of the reactivity of β-diketiminato magnesium and calcium complexes with Roesky's similarly coordinated aluminium(I) species, $[(^{Dipp}BDI)Al]$ (**2**).[4] Compound **2** reacts with $[(^{Dipp}BDI)MgMe]$, $[(^{Dipp}BDI)MgH]_2$ or $[(TMEDA)MgI_2]$ to provide the Mg-Al bonded oxidative addition products (e.g., **3** and **4**, Scheme 1).[5–7] In contrast, Harder has observed that addition of **2** to (^{Dipp}BDI)Ca-based reagents results in arene activation. While reaction with the ionic calcium complex $[(^{Dipp}BDI)Ca]^+[B(C_6F_5)_4]^-$ provided two electron reduction of benzene,[8] addition of **1** to benzene or toluene solutions of **2** resulted in arene C–H activation and the production of $[(^{Dipp}BDI)Al(H)Ar]$ complexes (Scheme 1).[6] Density functional theory (DFT) calculations of this latter reactivity implicated an initial Ca–Al bonded oxidative addition product, $[(^{Dipp}BDI)Al(H)Ca(^{Dipp}BDI)]$ (**5**), which, although otherwise analogous to compound **4**, is unobservable due to its rapid nucleophilic activation of the arene solvent.

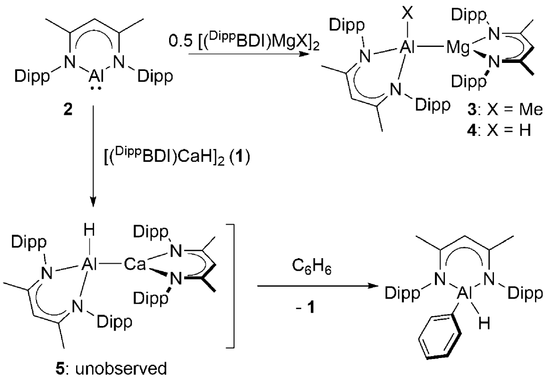

Scheme 1. Reactivity of compound **2** with (^{Dipp}BDI)Ae reagents.

While Scheme 1 highlights how the reactivity of a neutral Al^I nucleophile may be augmented by the presence of a calcium center, other recent advances have illuminated a further pathway to the formation of group 2 alumanyl derivatives. Building on the earlier development of boryl and gallyl nucleophiles,[9] the groups of Aldridge, Goicoechea and Coles have extended the range of *N*-heterocyclic group 13-centered anions to include the potassium alumanyl species, **6** and **7** (Figure 1).[10–14] The formally monovalent aluminum centers in both compounds can behave as potent reducing agents or as aluminum-centered nucleophiles. Of most relevance to these studies, the potassium reagent **6** can activate the C–H or C–C bonds of benzene, and reacts with $[(^{Mes}BDI)MgI(OEt_2)]$ ($^{Mes}BDI = HC\{(Me)CN$-2,4,6-

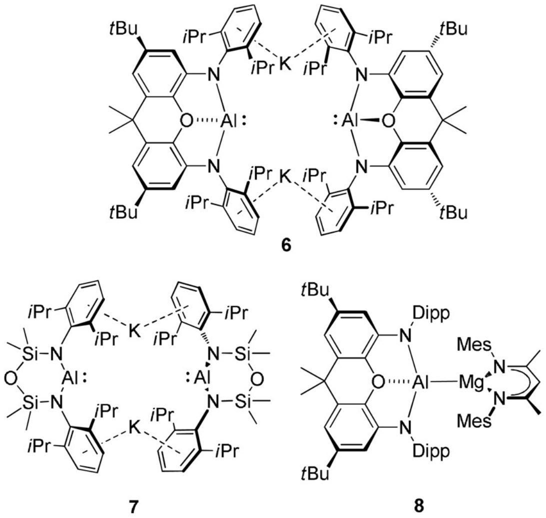

Figure 1. The potassium alumanyl derivatives, **6** and **7**, and the Al–Mg bonded species, **8**.

[*] Dr. R. J. Schwamm, Prof. M. S. Hill, Dr. M. F. Mahon, Dr. C. L. McMullin, Dr. N. A. Rajabi, Dr. A. S. S. Wilson
Department of Chemistry, University of Bath
Bath, BA2 7AY (UK)
E-mail: msh27@bath.ac.uk
cm2025@bath.ac.uk
Prof. M. P. Coles
School of Chemical and Physical Sciences
Victoria University of Wellington
PO Box 600, Wellington (New Zealand)

Supporting information and the ORCID identification number(s) for the author(s) of this article can be found under: https://doi.org/10.1002/anie.201914986.

$Me_3C_6H_2\}_2$) to yield a further Mg−Al bonded complex, **8** (Figure 1).[10,12] In contrast to this recent development of magnesium alumanyl chemistry, the gallyl derivatives of Jones and co-workers, *trans*-[Ca{Ga[(DippNCR)$_2$]}$_2$(THF)$_4$] (R = H, Me) and *trans*-[Ca{Ga(DippNCH)}$_2$(TMEDA)$_2$],[15] provide the only examples of isolable compounds containing calcium-group 13 σ-bonds and no calcium alumanyls have been considered beyond the implied intermediacy of species **5**.[6] In this contribution, therefore, and as an extension to our recent interest in the reactivity of alkaline earth boryls,[16] we describe a seven-membered cyclic alumanyl anion and its use in the synthesis of a stable, yet highly reactive, calcium derivative.

Following an analogous procedure to that employed in the synthesis of compound **7**,[13] addition of the pre-ligand {SiN^{Dipp}}H$_2$ (**9**, {SiN^{Dipp}} = {CH$_2$SiMe$_2$N(Dipp)}$_2$) to trimethylaluminum provided [{SiN^{Dipp}}AlMe] (**10**) (Scheme 2). The

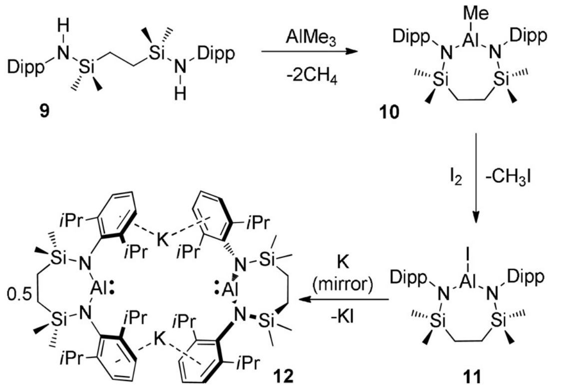

Scheme 2. Synthesis of compounds **10**–**12**.

slow conversion of **10** to [{SiN^{Dipp}}AlI] (**11**) was achieved by reaction with I$_2$, providing > 95 % conversion after 5 days at 100 °C. The solid-state structure of **11** was investigated by single crystal X-ray diffraction, confirming the formation of a 7-membered metallacycle via *N,N'*-chelation to a planar three-coordinate aluminum center [Al-N, 1.782(1) and 1.790(1); Al-I, 2.4690(5) Å] (Supporting Information, Figure S10).[20]

Stirring a solution of **11** in hexane over a potassium mirror resulted in a gradual change from colorless to yellow and the deposition of a grey solid. Filtration of the reaction mixture after 3 days at room temperature and removal of the volatile components gave a yellow powder, which crystallized from Et$_2$O to provide crystals of [Al{SiN^{Dipp}}K]$_2$ (**12**). The resultant ^{1}H and ^{13}C{^{1}H} NMR spectra were consistent with a symmetrical *N,N'*-chelated disposition of the diamide ligand about aluminum, a deduction confirmed by a subsequent single crystal X-ray diffraction analysis (Figure 2). Like both the previously reported derivatives, **6** and **7**,[10,13] the asymmetric unit of compound **12** comprises two "Al{SiN^{Dipp}}K" entities linked through flanking η^6-K⋯Ar interactions [range 2.945(1)–3.026(1) Å]. As expected for a lower oxidation state aluminum species, the Al−N bond distances [range 1.887(2)–1.892(2) Å] are significantly longer than those of **11**. Despite the larger bite angles imposed by chelation of the {SiN^{Dipp}}

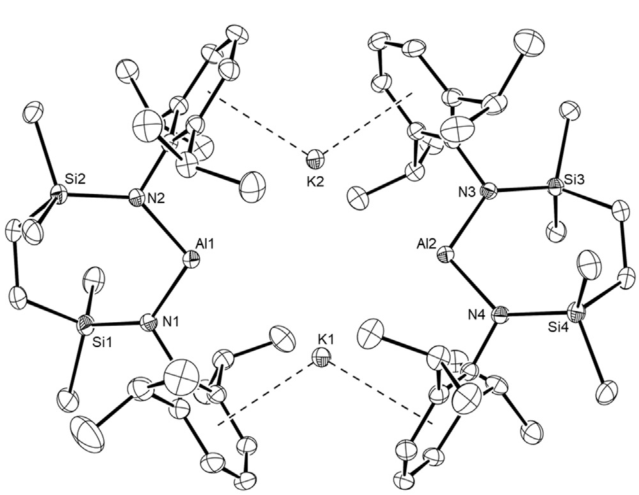

Figure 2. ORTEP representation of compound **12** (30 % probability ellipsoids). Hydrogen atoms and occluded molecule of diethyl ether solvent are omitted for clarity. Selected bond lengths [Å] and angles [°]: Al1−N1 1.887(2), Al1−N2 1.8889(19), Al2−N3 1.890(2), Al2−N4 1.892(2), Si1−N1 1.729(2), Si2−N2 1.7333(19), Si3−N3 1.731(2), Si4−N4 1.731(2); N1−Al1−N2 108.84(9), N3−Al2−N4 108.77(9).

ligand [**12**: N1−Al1−N2 108.84(9), N3−Al2−N4 108.77(9)° versus **7**: 103.89(8), 105.05(8)°], the Al⋯Al distance [5.721(1) Å] and Al⋯K distances [range 3.584(1)–3.625(1) Å] are also comparable to the analogous measurements within compound **7** [Al⋯Al 5.673(1); Al⋯K 3.5916(8) Å].

Although the implications of any metrical adjustments on the electronic structure of compound **12** will be addressed elsewhere, the similarity of its gross features to both compounds **6** and **7** advocates that **12** should display comparable reactivity. Mindful of Evans' use of tetraphenylborate derivatives of similarly electropositive rare earth elements as hydrocarbon-soluble reagents in further synthesis,[17] we prepared [(^{Dipp}BDI)AeBPh$_4$] (**13**, Ae = Mg; **14**, Ae = Ca) by the respective reactions of [(^{Dipp}BDI)Mg*n*-Bu] and [(^{Dipp}BDI)CaN(SiMe$_3$)$_2$] with [HNEt$_3$][BPh$_4$]. Both compounds **13** and **14** were isolated in high yields and their solid-state structures were confirmed by X-ray diffraction analysis (Figures S16 and S20) as mononuclear species in which the tetraphenylborate anions interact with the Ae centers via polyhapto Ae⋯μ−Ph−B interactions.

Addition of toluene solutions of compound **12** to either compound **13** or **14** resulted in a colorless suspension of KBPh$_4$ and, after crystallization from *n*-hexane and benzene, respectively, the formation of the magnesium and calcium alumanyl species, [{SiN^{Dipp}}Al-Mg(^{Dipp}BDI)] (**15**) and [{SiN^{Dipp}}Al-Ca(^{Dipp}BDI)] (**16**), as colorless and yellow crystals (Scheme 3). The solid-state structures of both compounds **15** and **16** were determined by X-ray diffraction analysis, which confirmed them as magnesium and calcium derivatives comprising aluminum to alkaline earth interactions.

Both the Mg1 and Al1 centers of compound **15** are unambiguously three-coordinate (closest Al−C separation 4.965 Å) and the two *N*-donor ligand systems are almost orthogonal (Figure 3 a), such that the dihedral angle subtended by the N1−Al1−N2 and N3−Mg1−N4 mean planes is 84.1°. Although the Mg1-Al1 bond in **15** [2.7980(6) Å] is

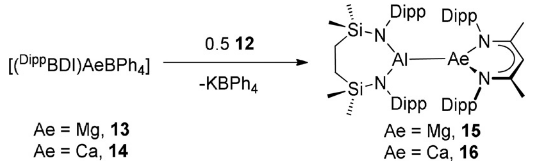

Scheme 3. Synthesis of the magnesium and calcium alumanyl compounds, **15** and **16**.

longer than the comparable length in compound **8** [2.696(1) Å],[10] it is commensurate with the corresponding distances observed in compounds **3** [2.7687(8) Å] and **4** [2.7687(5) Å],[5,6] which also comprise magnesium coordinated by the ^{Dipp}BDI ligand, and in Jones' derivative, [(TMEDA)(I)Mg-Al(I)(^{Dipp}BDI)] [2.727(2) Å].[7]

Like **15**, compound **16** contains a direct alkaline earth to aluminum bond (Figure 3b). Although the Al−Ca bond length [3.1664(4) Å] is 6.6% longer than the sum of covalent radii of the metal centers, this distance is closely comparable with that calculated for the analogous intermetallic separation [3.120 Å] in the unobservable intermediate **5** (Scheme 1).

The coordination sphere of Ca1 is augmented by a pronounced η^6-interaction with the C1-C6-containing Dipp substituent [Ca1−C range; 2.9790(17)–3.2215(15) Å] of the aluminum-coordinated diamide ligand. The consequent asymmetry in the relative orientation of the {SiN^{Dipp}}Al and (^{Dipp}BDI)Ca units is particularly reflected by the N1−Al−Ca1 [98.14(4)°] and N2−Al1−Ca1 [150.30(5)°] angles.

Insight into the contrasting structures of **15** and **16** was provided by DFT calculations.[18] Both structures optimized to geometries close to those in the solid state, albeit with slightly overestimated metal-metal bond lengths (**15**, Mg−Al 2.85; **16**, Ca-Al 3.25 Å). Inspection of the localised Pipek–Mezey orbitals for compounds **15** and **16** (Figures 4a,b) emphasizes the polarization intrinsic to both the Al−Mg and Al−Ca σ-bonds. Although contributions from the aluminum centers dominate both orbitals, the charge distributions clearly reflect the greater ionic character of the Al−Ca interaction, an observation further underscored by the calculated NBO charges (**15**, Mg +1.45 Al +0.83; **16** Ca +1.65, Al +0.72 a.u.). Similarly, QTAIM plots of **15** and **16** identify bond critical points (BCPs) on both Ae−Al bond paths (Figures 4c,d). The attributes of the BCP associated with the Al−Mg bond path [higher $\rho(r)$, 0.028 a.u. (**15**) versus 0.020 (**16**) and more negative H(r), −0.008 a.u. (**15**) versus −0.002 a.u. (**16**)], however, are indicative of a marginally higher covalency between magnesium and aluminum than for the equivalent Al−Ca interaction. Although compound **16** features a further bond path between the Ca center and a Dipp substituent of the {SiN^{Dipp}}Al unit, this BCP is characterized by a very small $\rho(r)$ and small positive H(r). Similarly, analysis of the relevant NBOs of **16** (HOMO-8 and HOMO-10, Figure S37) and visualization of the analogous non covalent interaction (NCI) index (Figure S39) indictate that this interaction is non-covalent in origin and only weakly stabilizing of the structure as a whole.

Preliminary investigations indicate that compound **16** provides a significantly enhanced source of reactivity in comparison to its lighter analogue. While neither compound displays any observable reaction with benzene or toluene, and compound **15** is stable in ether solvents, addition of THF to a solution of compound **16** in methylcyclohexane resulted in

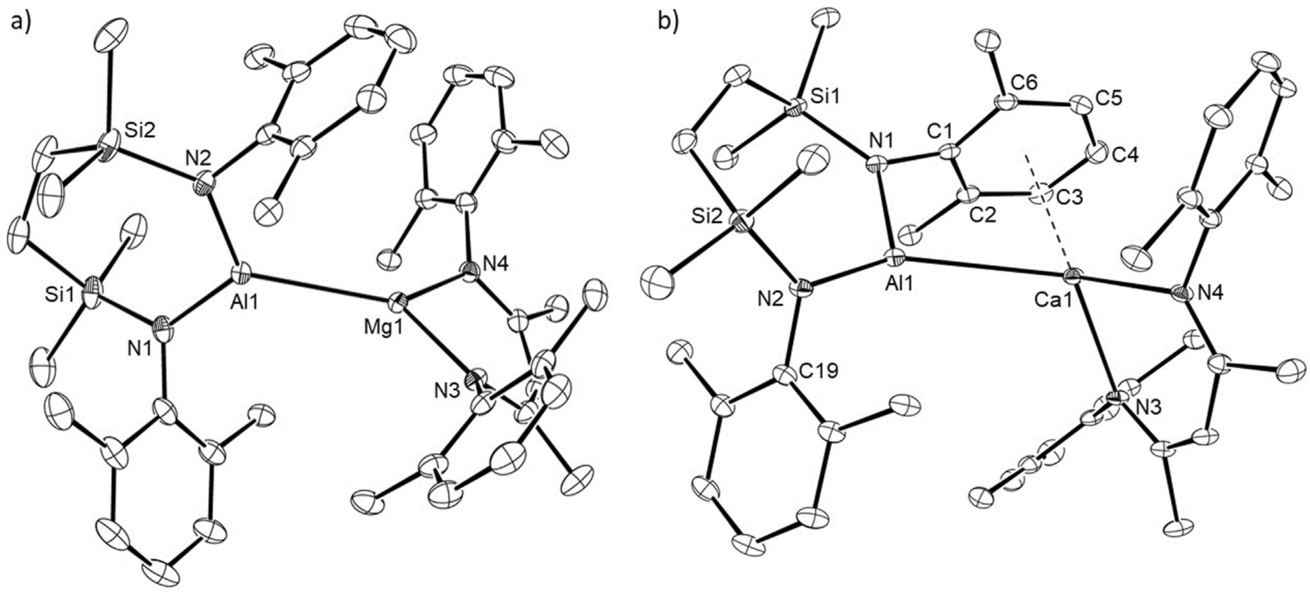

Figure 3. ORTEP representations of a) compound **15** and b) compound **16** (30% probability ellipsoids). Hydrogen atoms, *iso*-propyl carbon atoms and disordered molecules of solvent are omitted for clarity. Selected bond lengths [Å] and angles [°]: (**15**) Al1−Mg1 2.7980(6), Al1−N1 1.8482(13), Al1−N2 1.8402(13), Mg1−N3 2.0528(12), Mg1−N4 2.0721(12); N1−Al1−Mg1 125.94(5), N2−Al1−Mg1 121.91(4), N2−Al1−N1 111.87(6), N3−Mg1−Al1 132.59(4), N3−Mg1−N4 93.77(5), N4−Mg1−Al1 132.94(4); (**16**) Ca1−Al1 3.1229(5), Al1−N1 1.8973(13), Al1−N2 1.8544(14), Ca1−N3 2.3538(12), Ca1−N4 2.3682(13), Ca1−C1 3.1735(15), Ca1−C2 3.1333(16), Ca1−C3 3.0213(17), Ca1−C4 2.9790(17), Ca1−C5 3.0884(16), Ca1−C6 3.2215(15); N2−Al1−N1 111.08(6), N3−Ca1−N4 81.10(4), N1−Al1−Ca1 98.14(4), N2−Al1−Ca1 150.30(5), N3−Ca1−Al1 118.99(3), N4−Ca1−Al1 123.45(3).

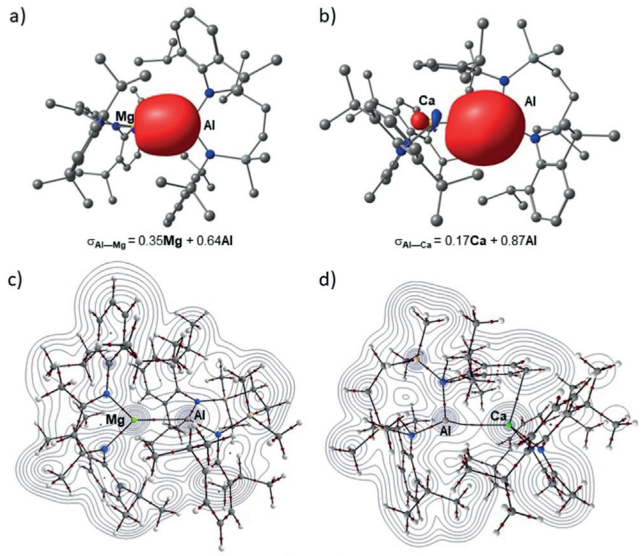

BCP	ρ(r)	$\nabla^2\rho(r)$	ε	H(r)
Mg—Al	**0.028**	+0.033	0.049	-0.008

BCP	ρ(r)	$\nabla^2\rho(r)$	ε	H(r)
Ca—Al	**0.020**	+0.020	0.052	-0.002
Ca—C_a	**0.014**	+0.051	1.125	+0.015

Figure 4. Localized Pipek–Mezey orbitals of a) **15** and b) **16** showing Al—Ca and Al—Mg σ-bonding orbitals, respectively. QTAIM molecular graphs of c) **15** and d) **16**. The electron density contours are computed in the {Mg/Al/Si} planes with bond critical points (BCPs) shown as small red spheres. BCP electron densities ($\rho(r)$ in e Å^{-3}), values of the Laplacian of the electron density ($\nabla^2\rho(r)$ in e Å^{-5}), ellipticities (ε) and total energy densities (H(r) in a.u.) are tabulated beneath the relevant figures.

the immediate decoloration of the yellow solution and the formation of a single new compound (**17**). The ionic complex **17** comprises a charge separated $[(^{Dipp}BDI)Ca(THF)_3]^+$ cation and an aluminate anion (Figure 5a), which may be considered as the formal product of oxidative addition of a THF C—O bond to the aluminum(I) center of the $[\{SiN^{Dipp}\}Al]^-$ anion.[19] Similarly, compound **15** is unreactive toward 1,3,5,7-cyclooctatetraene (COT), whilst addition of COT to compound **16** results in its two-electron aromatization and production of the asymmetric and heterobimetallic inverse sandwich species, compound **18** (Figure 5b). Although the chemistry of compounds **17**, **18** and related derivatives will be discussed in detail elsewhere, these initial observations confirm that such heavier alkaline earth alumanyls, like group 2 organoderivatives, may provide a source of striking and unprecedented reactivity. We are continuing to elaborate these possibilities.

Acknowledgements

We thank the Royal Commission for the Exhibition of 1851 for the provision of a Postdoctoral Fellowship (RJS) and the EPSRC (EP/R020752/1) for support of this research. This research made use of the Balena High Performance Computing (HPC) Service at the University of Bath.

Conflict of interest

The authors declare no conflict of interest.

Keywords: alumanyl · calcium · density functional theory · magnesium · potassium

How to cite: *Angew. Chem. Int. Ed.* **2020**, *59*, 3928–3932
Angew. Chem. **2020**, *132*, 3956–3960

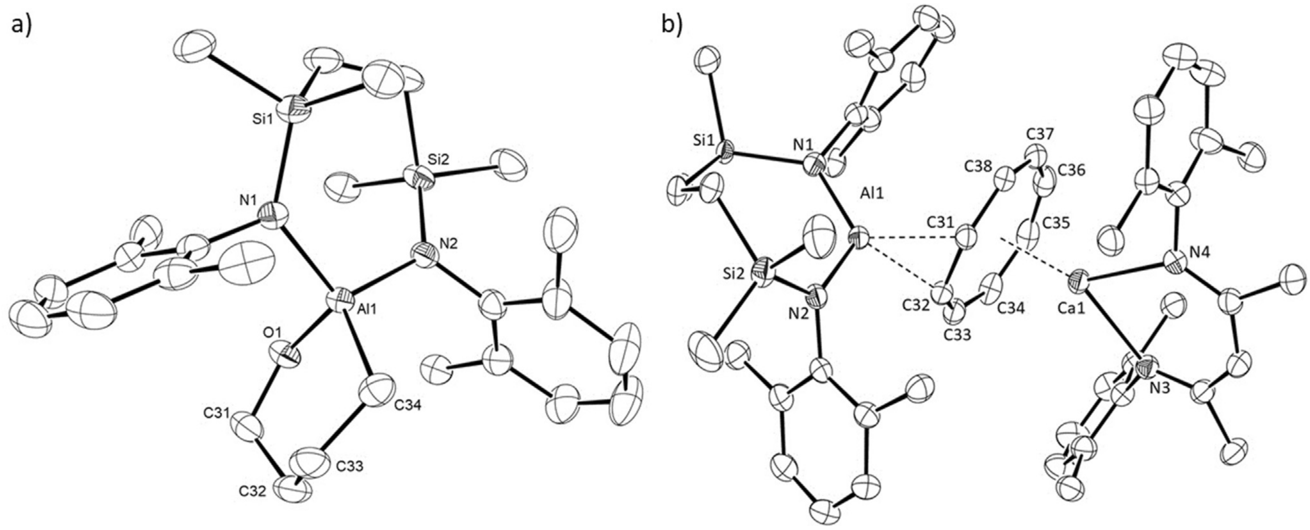

Figure 5. ORTEP representations of (a) the aluminate component of compound **17** and (b) compound **18** (30% probability ellipsoids). Hydrogen atoms and *iso*-propyl carbon atoms, in both structures, and a disordered molecule of benzene solvent in **18** are omitted for clarity. Selected bond lengths [Å] and angles [°]: (**17**) Al1—O1 1.7637(16), Al1—N1 1.8997(18), Al1—N2 1.889(2), Al1—34 1.984(3); O1—Al1—N1 109.88(8), O1—Al1—N2 106.51(8), O1—Al1—C34 102.23(10), N1—Al1—C34 113.76(10), N2—Al1—N1 110.75(8), N2—Al1—C34 113.10(10); (**18**) Al1—N1 1.8085(17), Al1—N2 1.8200(16), Al1—C31 2.125(2), Al1—C32 2.123(2), Ca1—N3 2.3437(17), Ca1—N4 2.3831(18), Ca1—C31 2.7107(19), Ca1—C32 2.804(2), Ca1—C33 2.818(2), Ca1—C34 2.753(2), Ca1—35 2.693(2), Ca1—C36 2.695(2), Ca1—C37 2.706(2), Ca1—C38 2.698(2); N1—Al1—N2 119.27(8), N3—Ca1—N4 79.34(6).

[1] a) M. S. Hill, D. J. Liptrot, C. Weetman, *Chem. Soc. Rev.* **2016**, *45*, 972 – 988; b) Y. Sarazin, J. F. Carpentier, *Chem. Rec.* **2016**, *16*, 2482 – 2505; c) M. R. Crimmin, M. S. Hill in *Alkaline-Earth Metal Compounds: Oddities and Applications*, *Vol. 45* (Ed.: S. Harder), Springer, Heibelberg, **2013**, pp. 191 – 241; d) S. Harder, *Chem. Rev.* **2010**, *110*, 3852 – 3876; e) A. G. M. Barrett, M. R. Crimmin, M. S. Hill, P. A. Procopiou, *Proc. R. Soc. London Ser. A* **2010**, *466*, 927 – 963.

[2] a) D. Mukherjee, J. Okuda, *Angew. Chem. Int. Ed.* **2018**, *57*, 1458 – 1473; *Angew. Chem.* **2018**, *130*, 1472 – 1488; b) D. Mukherjee, D. Schuhknecht, J. Okuda, *Angew. Chem. Int. Ed.* **2018**, *57*, 9590 – 9602; *Angew. Chem.* **2018**, *130*, 9736 – 9749; c) S. Harder, *Chem. Commun.* **2012**, *48*, 11165 – 11177.

[3] a) A. S. S. Wilson, M. S. Hill, M. F. Mahon, C. Dinoi, L. Maron, *Science* **2017**, *358*, 1168 – 1171; b) A. S. S. Wilson, C. Dinoi, M. S. Hill, M. F. Mahon, L. Maron, *Angew. Chem. Int. Ed.* **2018**, *57*, 15500 – 15504; *Angew. Chem.* **2018**, *130*, 15726 – 15730; c) A. S. S. Wilson, M. S. Hill, M. F. Mahon, *Organometallics* **2019**, *38*, 351 – 360.

[4] C. M. Cui, H. W. Roesky, H. G. Schmidt, M. Noltemeyer, H. J. Hao, F. Cimpoesu, *Angew. Chem. Int. Ed.* **2000**, *39*, 4274 – 4276; *Angew. Chem.* **2000**, *112*, 4444 – 4446.

[5] C. Bakewell, B. J. Ward, A. J. P. White, M. R. Crimmin, *Chem. Sci.* **2018**, *9*, 2348 – 2356.

[6] S. Brand, H. Elsen, J. Langer, S. Grams, S. Harder, *Angew. Chem. Int. Ed.* **2019**, *58*, 15496 – 15503; *Angew. Chem.* **2019**, *131*, 15642 – 15649.

[7] A. Paparo, C. D. Smith, C. Jones, *Angew. Chem. Int. Ed.* **2019**, *58*, 11459 – 11463; *Angew. Chem.* **2019**, *131*, 11581 – 11585.

[8] S. Brand, H. Elsen, J. Langer, W. A. Donaubauer, F. Hampel, S. Harder, *Angew. Chem. Int. Ed.* **2018**, *57*, 14169 – 14173; *Angew. Chem.* **2018**, *130*, 14365 – 14369.

[9] a) E. S. Schmidt, A. Jockisch, H. Schmidbaur, *J. Am. Chem. Soc.* **1999**, *121*, 9758 – 9759; b) R. J. Baker, R. D. Farley, C. Jones, M. Kloth, D. M. Murphy, *J. Chem. Soc. Dalton Trans.* **2002**, 3844 – 3850; c) Y. Segawa, M. Yamashita, K. Nozaki, *Science* **2006**, *314*, 113 – 115; d) M. Yamashita, K. Nozaki in *Synthesis and Application of Organoboron Compounds*, *Vol. 49* (Eds.: E. Fernandez, A. Whiting), Springer, Heidelberg, **2015**, pp. 1 – 37.

[10] J. Hicks, P. Vasko, J. M. Goicoechea, S. Aldridge, *Nature* **2018**, *557*, 92 – 95.

[11] J. Hicks, A. Mansikkamaki, P. Vasko, J. M. Goicoechea, S. Aldridge, *Nat. Chem.* **2019**, *11*, 237 – 241.

[12] J. Hicks, P. Vasko, J. M. Goicoechea, S. Aldridge, *J. Am. Chem. Soc.* **2019**, *141*, 11000 – 11003.

[13] R. J. Schwamm, M. D. Anker, M. Lein, M. P. Coles, *Angew. Chem. Int. Ed.* **2019**, *58*, 1489 – 1493; *Angew. Chem.* **2019**, *131*, 1503 – 1507.

[14] A dialkyl-substituted alumanyl anion has also very recently been described; S. Kurumada, S. Takamori, M. Yamashita, *Nat. Chem.* **2019**, *12*, 36 – 39..

[15] C. Jones, D. P. Mills, J. A. Platts, R. P. Rose, *Inorg. Chem.* **2006**, *45*, 3146 – 3148; O. Bonello, C. Jones, A. Stasch, W. D. Woodul, *Organometallics* **2010**, *29*, 4914 – 4922.

[16] a) A. F. Pécharman, A. L. Colebatch, M. S. Hill, C. L. McMullin, M. F. Mahon, C. Weetman, *Nat. Commun.* **2017**, *8*, 15022; b) A. F. Pécharman, M. S. Hill, C. L. McMullin, M. F. Mahon, *Angew. Chem. Int. Ed.* **2017**, *56*, 16363 – 16366; *Angew. Chem.* **2017**, *129*, 16581 – 16584; c) A. F. Pécharman, N. A. Rajabi, M. S. Hill, C. L. McMullin, M. F. Mahon, *Chem. Commun.* **2019**, *55*, 9035 – 9038; d) A. F. Pécharman, M. S. Hill, G. McMullon, C. L. McMullin, M. F. Mahon, *Chem. Sci.* **2019**, *10*, 6672 – 6682.

[17] W. J. Evans, C. A. Seibel, J. W. Ziller, *J. Am. Chem. Soc.* **1998**, *120*, 6745 – 6752.

[18] The BP86 functional was used for optimizations, with Mg, Al, Si and Ca centres described with the Stuttgart RECPs and 6-31G** basis set for all other atoms. Further and more detailed information regarding the methodology can be found in the Supporting Information.

[19] Analogous reactivity with THF at either the isolated Al^{I} center of compound **2** or during attempted reduction of Al^{III} has previously been observed in a) T. Chu, Y. Boyoko, I. Korobkov, G. Nikonov, *Organometallics* **2015**, *34*, 5363 – 5365; b) C. Schnitter, H. W. Roesky, C. Röpken, R. Herbst-Irmer, H.-G. Schmidt, M. Noltemeyer, *Angew. Chem. Int. Ed.* **1998**, *37*, 1952 – 1955; *Angew. Chem.* **1998**, *110*, 2059 – 2062; c) M. Schormann, K. S. Klimek, H. Hatop, S. P. Varkey, H. W. Roesky, C. Lehmann, C. Röpken, R. Herbst-Irmer, H.-G. Schmidt, M. Noltemeyer, *J. Solid State Chem.* **2001**, *162*, 225 – 236.

[20] CCDC 1967220, 1967221, 1967222, 1967223, 1967224, 1967225, 1967226, 1967227 and 1967228 contain the supplementary crystallographic data for this paper. These data can be obtained free of charge from The Cambridge Crystallographic Data Centre.

Manuscript received: November 24, 2019
Accepted manuscript online: December 12, 2019
Version of record online: January 30, 2020

